NACA TN 3576

NATIONAL ADVISORY COMMITTEE FOR AERONAUTICS

TECHNICAL NOTE 3576

FURTHER MEASUREMENTS OF INTENSITY, SCALE, AND SPECTRA OF TURBULENCE IN A SUBSONIC JET

By James C. Laurence and Truman M. Stickney

Lewis Flight Propulsion Laboratory
Cleveland, Ohio

Washington

October 1956

NATIONAL ADVISORY COMMITTEE FOR AERONAUTICS

TECHNICAL NOTE 3576

FURTHER MEASUREMENTS OF INTENSITY, SCALE, AND SPECTRA OF TURBULENCE IN A SUBSONIC JET

By James C. Laurence and Truman M. Stickney

SUMMARY

As an extension to the data reported in Technical Note 3561, hot-wire-anemometer measurements of the intensity, scale, and spectra of turbulence in a 3.5-inch-diameter free subsonic jet were made for downstream distances from 8 to 20 jet diameters. The results show that the eddy size increased with distance from the jet nozzle until a maximum was reached. The position of this maximum depended upon the distance from the jet centerline. After reaching the maximum, the eddy decreased uniformly in size with distance from the nozzle.

The nondimensional mean-velocity profiles were nearly similar in a region from 12 to 20 jet diameters from the nozzle. Corresponding similarity in intensity of turbulence profiles, however, was not observed as far as 20 jet diameters downstream of the nozzle.

INTRODUCTION

The results of hot-wire-anemometer surveys in a 3.5-inch-diameter free subsonic jet are presented in reference 1 for axial distances not greater than 8 jet diameters downstream of the jet nozzle. As was explained there, the increasing interest in the problem of reducing the noise of jets has made more turbulence data necessary.

A continuation of the jet studies at the NACA Lewis laboratory has resulted in the completion of the turbulence surveys to about 20 jet diameters downstream of the jet nozzle. This work was done as part of the jet-noise program in order to further the efforts that are being made to correlate turbulence and noise.

The experimental methods explained in reference 1 - in particular, the use of the autocorrelation technique - are considered especially useful in turbulence studies, because they show that the turbulence eddy does not change appreciably during the short time or space interval

considered. In addition, improvements in the correlation computer have further simplified the job of extensive turbulence surveys.

In this report, as in reference 1, constant-temperature hot-wire anemometers were used to obtain the intensity, the scale, the spectra, and the velocity autocorrelations at points distributed throughout the jet. The points considered ranged from axial distances of 8 to 20 jet diameters downstream of the nozzle and were uniformly distributed across the turbulent jet from the centerline to the outer boundaries. Since the jet was found to be symmetrical about the axis, only one-half of the complete jet was explored.

In reference 1 it is shown that variations in jet speed (Mach and/or Reynolds number) have only small effects on these turbulence parameters. In addition, turbulence studies in water (ref. 2), which show results similar to those in air, tend to confirm that the observed effects are Reynolds number effects. Hence, the turbulent velocity measurements were conducted at a core Reynolds number of 300,000 (based on jet radius) and a Mach number of 0.3.

INSTRUMENTATION AND TEST PROCEDURES

The instrumentation and test procedures in this report are those which were used in reference 1. The hot-wire anemometers are the constant-temperature type described in reference 3. The hot-wire signals were recorded in three ways at each point in the jet stream (see fig. 1):

(1) The root-mean-square value of the wire voltage fluctuations was read from an rms voltmeter.

(2) The spectrum of the wire voltages was recorded by the spectrum analyzer.

(3) The wire voltage fluctuations were recorded on magnetic tape for later processing with the computer.

The correlation computer used in this work is described in reference 4. The signal from a single hot-wire anemometer is recorded simultaneously on two channels of a magnetic tape recorder. At playback, one of the signals can be delayed with respect to the other by moving one of the pickup heads. Thus, two signals are obtained which are segments of the same signal separated in time. Upon processing, these two signals lead

to an autocorrelation coefficient defined as $\frac{\overline{e_t e_{t+\Delta t}}}{\sqrt{\overline{e_t^2}}\sqrt{\overline{e_{t+\Delta t}^2}}}$, which was shown in reference 1 to be $\frac{\overline{u_t u_{t+\Delta t}}}{\sqrt{\overline{u_t^2}}\sqrt{\overline{u_{t+\Delta t}^2}}}$.

The free jet used is the same 3.5-inch-diameter jet described in reference 1 and the mean flow and temperature instrumentation are also the same.

RESULTS AND DISCUSSION

The results of the experiments described in this report are presented in a series of graphs.

The mean-velocity profiles obtained from total-pressure surveys are shown in figure 2. In this figure the ratio of the local mean velocity to the mean core velocity is plotted against the dimensionless distance from the jet centerline in terms of jet radius. In each part of figure 2 the velocity ratios for the Mach numbers 0.2, 0.3, 0.5, and 0.7 are plotted for the corresponding Reynolds numbers of 192,000, 300,000, 500,000, and 725,000.

It is possible to plot the data for the mean flow to show the similarity of all the profiles in the completely developed flow region of the jet. In figure 3, the ratio of the local velocity to the maximum velocity (the velocity on the jet centerline) is plotted against a nondimensional mixing-zone width $y/y_{1/2}$. Similar data from references 5 and 6 are shown on this figure for comparison. The data of all these experiments fall closely about the line obtained from momentum transfer theory (ref. 7).

These additional data along with the data of reference 1 make it possible to define the approximate mean-flow jet boundaries. This has been done in figure 4, in which the effect of the potential core Mach number on the jet boundaries is shown.

In the turbulence intensity profiles (figs. 5 and 6), the intensity of the longitudinal component of the turbulent velocities in percent of core velocity is plotted against the nondimensional distance from the jet centerline. Figure 6 is plotted as percent of turbulence against a nondimensional mixing-zone width. In figure 6(a) the profiles near the jet nozzle are shown to be nearly similar, but this similarity disappears with the disappearance of the central core. The degree to which similarity has redeveloped downstream is shown in figure 6(b), where similarity is found only for points removed from the jet axis.

The results of the spectral density studies are shown in figures 7 and 8. The hot-wire voltages were analyzed by a spectrum analyzer with a band pass of constant percentage width. Here the coordinates are the spectral density (sec) plotted as a function of the frequency (cps). In figure 7 the spectra are given for distances from the jet nozzle x/r of 16, 24, 32, and 40 and the distance from the jet centerline $y/r = 1.028$; while in figure 8 spectra are given for $x/r = 32$ and y/r values of 0, 0.343, 1.028, 1.715, 2.400, 3.088, 3.772, 4.460, and 5.143. Faired curves are drawn through the data points.

The graphs of figure 7 show a progressive shift in energy level to the low-frequency components as the x/r values increase from 16 to 40. The graphs of figure 8, however, show very little change as the mixing zone is traversed.

The autocorrelation curves for the same points as for the spectra are presented in figures 9 and 10. The autocorrelation curves were obtained by means of a special correlation computer as explained in reference 1.

In reference 1 spectral density curves similar to those in figures 7 and 8 and both longitudinal correlation and autocorrelation curves were used to evaluate the scale of turbulence (ref. 8) defined as

$$L_X = \int_0^\infty R_X \, d_X$$

This method was not used in this report because no longitudinal correlations were measured and some of the autocorrelation coefficients were negative.

In order to arrive at an average eddy size from the experimental data, the spectral density curves were used. The method of obtaining the scale was similar to the one proposed by von Kármán (ref. 9) and used by Corrsin (ref. 6). The experimental points of the spectral density curves were fitted with an expression of the type

$$F(n) = \frac{K}{(1 + \pi^2 K^2 n^2)^{5/6}} \qquad (1)$$

in order to extrapolate the $F(n)$ curve to zero frequency. Figure 11 shows the result of fitting the data with a curve of the form of equation (1) for frequencies of 500 cps and less. The fit is seen to be adequate.

This method was used in this report to obtain the scale from the relation

$$L_x = \frac{F(0)U_l}{4}$$

Figure 12(a) shows the values of the longitudinal scale, as evaluated by this method, plotted as a function of the distance from the jet nozzle. This map of the scale of the turbulence of the subsonic jet may be useful in calculations of the aerodynamic noise of the jet. Figure 12(b) is a cross plot of figure 12(a).

If this scale is related to the average longitudinal size of the eddies in the turbulent flow, figure 12 shows that:

(1) The eddy size is a function of the distance from the jet nozzle.

(2) As the distance from the jet centerline is increased, the maximum eddy size occurs farther downstream.

(3) The maximum eddy size at distances downstream greater than 8 jet diameters occurs on the jet centerline.

CONCLUSIONS

Hot-wire anemometer measurements are reported for distances greater than 8 diameters from the exit nozzle of a subsonic jet. These results are obtained from a continuation of the program described in Technical Note 3561.

The intensity of turbulence expressed as a percent of the core velocity of the jet is given for a large number of points located within the jet. The intensity profiles show a development of similarity as the distance from the jet nozzle is increased with the location of the maximum intensity moving out from the jet centerline.

The spectra of the turbulence were used to obtain a longitudinal scale of the turbulence.

The longitudinal scale of the turbulence increases with distance from the jet nozzle with the maximum value of scale occurring at greater distances from the exit as the distance from the centerline is increased.

Mean velocity profiles are shown and are used to define the limits of the subsonic jet over a range of Mach numbers from 0.2 to 0.7.

Lewis Flight Propulsion Laboratory
National Advisory Committee for Aeronatuics
Cleveland, Ohio, April 24, 1956

APPENDIX - SYMBOLS

e	fluctuating component of hot-wire voltage
F(n)	spectral density function
K	constant
L	scale of turbulence
n	frequency
R	correlation coefficient
r	jet-nozzle radius
U	mean stream velocity
u	fluctuating component of velocity in x-direction
x,y	right-hand coordinate system with x-axis coinciding with centerline of jet
Δt	delay time

Subscripts:

c	core
l	local
max	maximum (on jet centerline)
t	time
x	longitudinal
Δt	delay time
1/2	points where local velocity is one-half the maximum or centerline velocity

Superscripts:

$\bar{}$	average
'	root-mean-square

REFERENCES

1. Laurence, James C.: Intensity, Scale, and Spectra of Turbulence in Mixing Region of Free Subsonic Jet. NACA TN 3561, 1955.

2. Forstall, Walton, and Gaylord, E. W.: Momentum and Mass Transfer in a Submerged Water Jet. Jour. Appl. Mech., vol. 22, no. 2, June 1955, pp. 161-164.

3. Laurence, James C., and Landes, L. Gene: Auxiliary Equipment and Techniques for Adapting the Constant-Temperature Hot-Wire Anemometer to Specific Problems in Air-Flow Measurements. NACA TN 2843, 1952.

4. Callaghan, Edmund E., Howes, Walton L., and Coles, Willard D.: Near Noise Field of a Jet-Engine Exhaust. II - Cross Correlation of Sound Pressures. NACA TN 3764, 1956.

5. Taylor, John F., Grimmett, H. L., and Comings, E. W.: Turbulent Mixing in an Isothermal Free Jet. Tech. Rep. No. 2, Univ. of Ill., Nov. 15, 1948. (Contract N6-ori-71, Task Order XI, Office Naval Res., Navy Dept.)

6. Corrsin, Stanley: Investigation of Flow in Axially Symmetric Heated Jet of Air. NACA WR W-94, 1943. (Supersedes NACA ACR 3L23.)

7. Pai, Shih-I.: Fluid Dynamics of Jets. D. Van Nostrand Co., Inc., 1954.

8. Taylor, G. I.: The Spectrum of Turbulence. Proc. Roy. Soc. (London), ser. A, vol. 164, Feb. 18, 1938, pp. 476-490.

9. von Kármán, Theodore: Progress in the Statistical Theory of Turbulence. Proc. Nat. Acad. Sci., vol. 34, no. 11, Nov. 15, 1948, pp. 530-539.

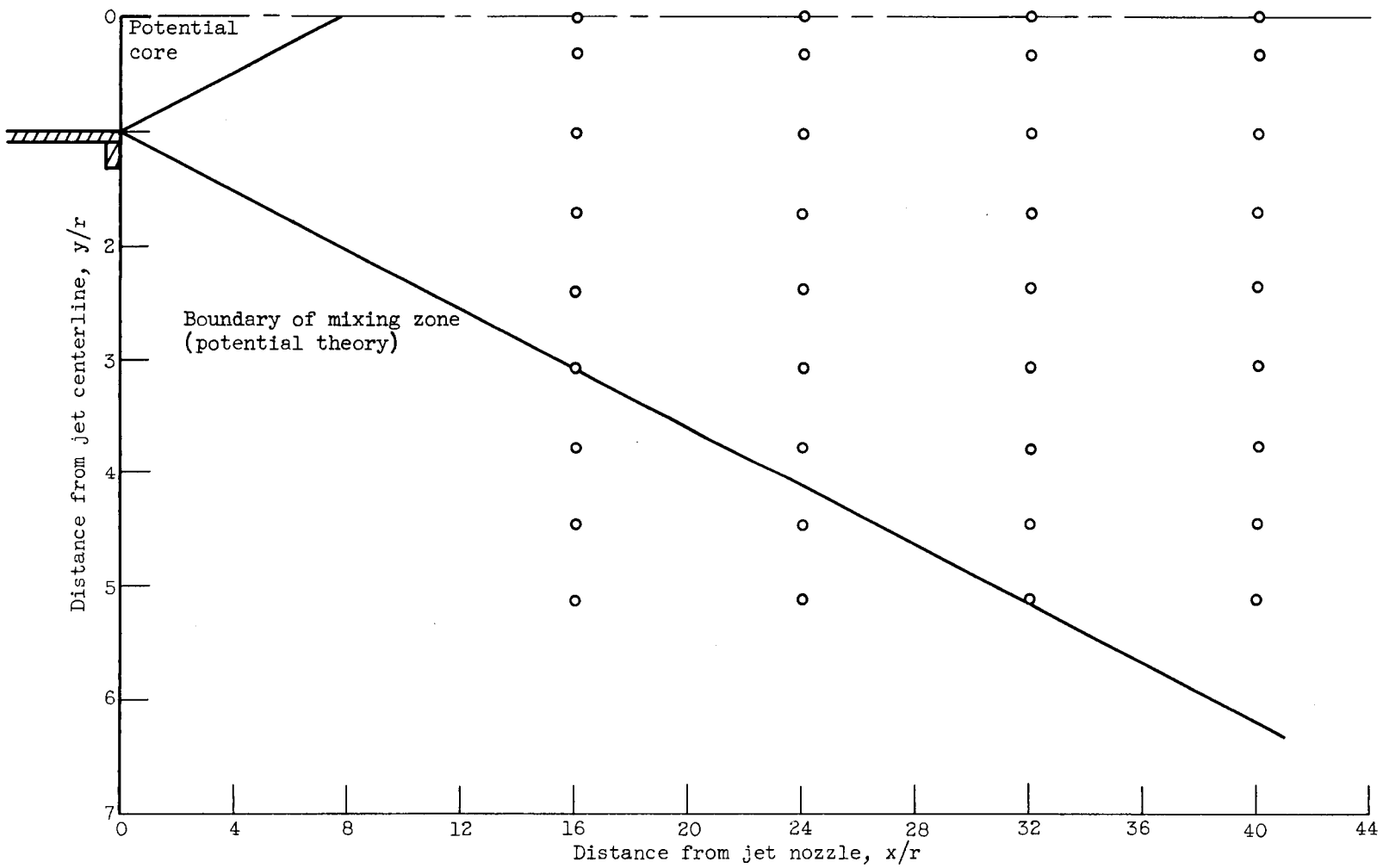

Figure 1. - Location of test points in subsonic jet.

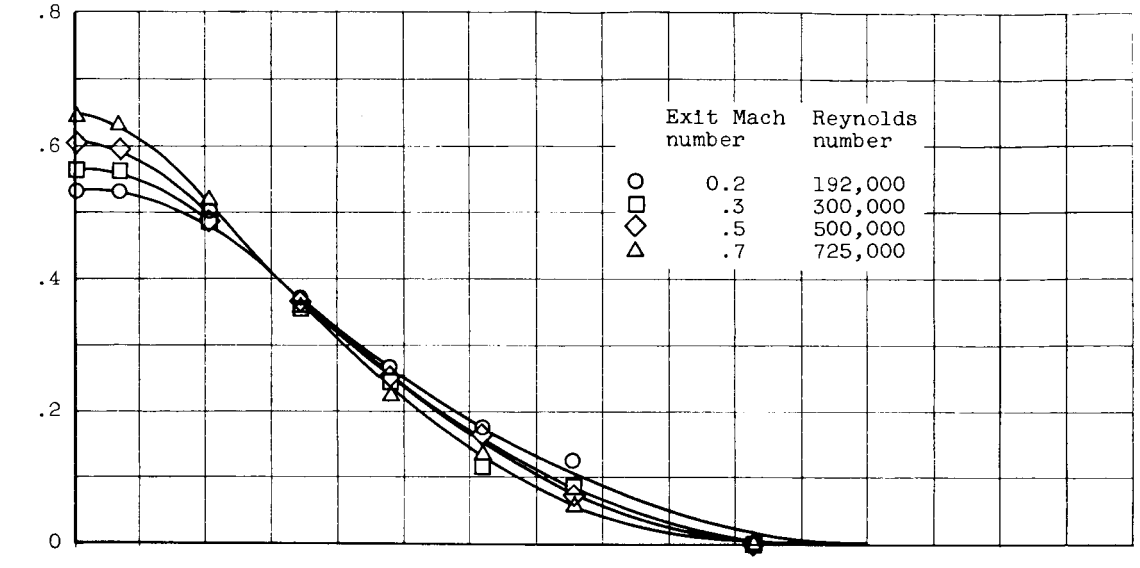

(a) Distance from jet nozzle x/r, 24.

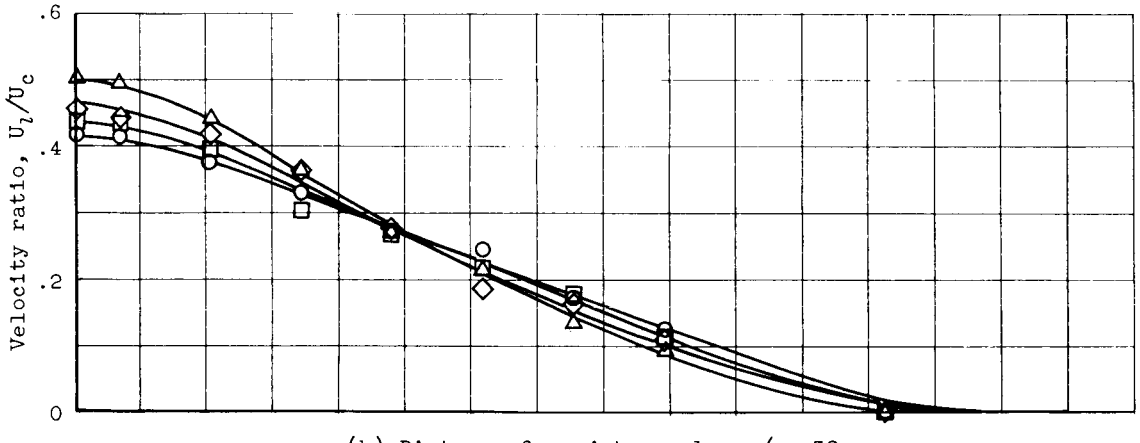

(b) Distance from jet nozzle x/r, 32.

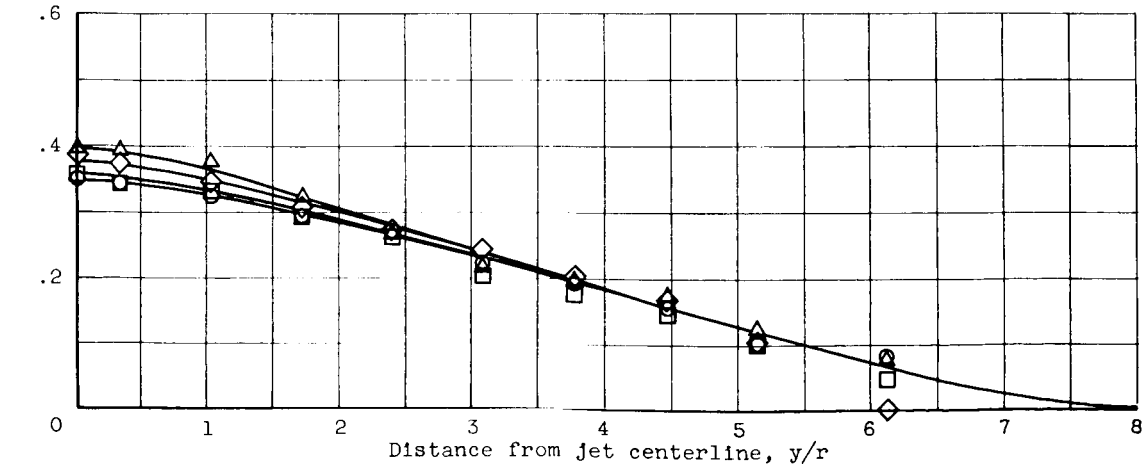

(c) Distance from jet nozzle x/r, 40.

Figure 2. - Mean-velocity profiles.

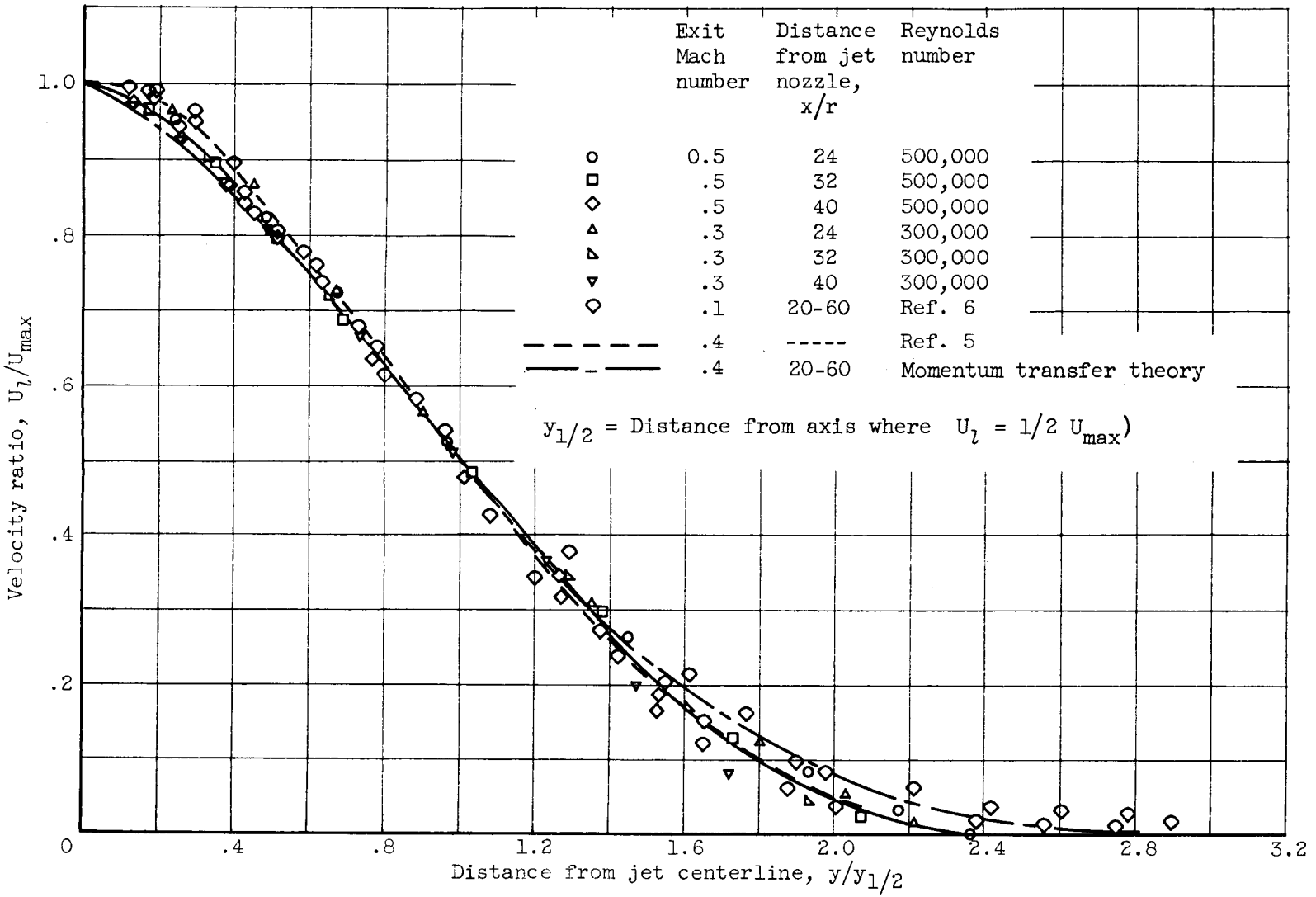

Figure 3. - Similarity of mean velocity profiles in fully developed flow region.

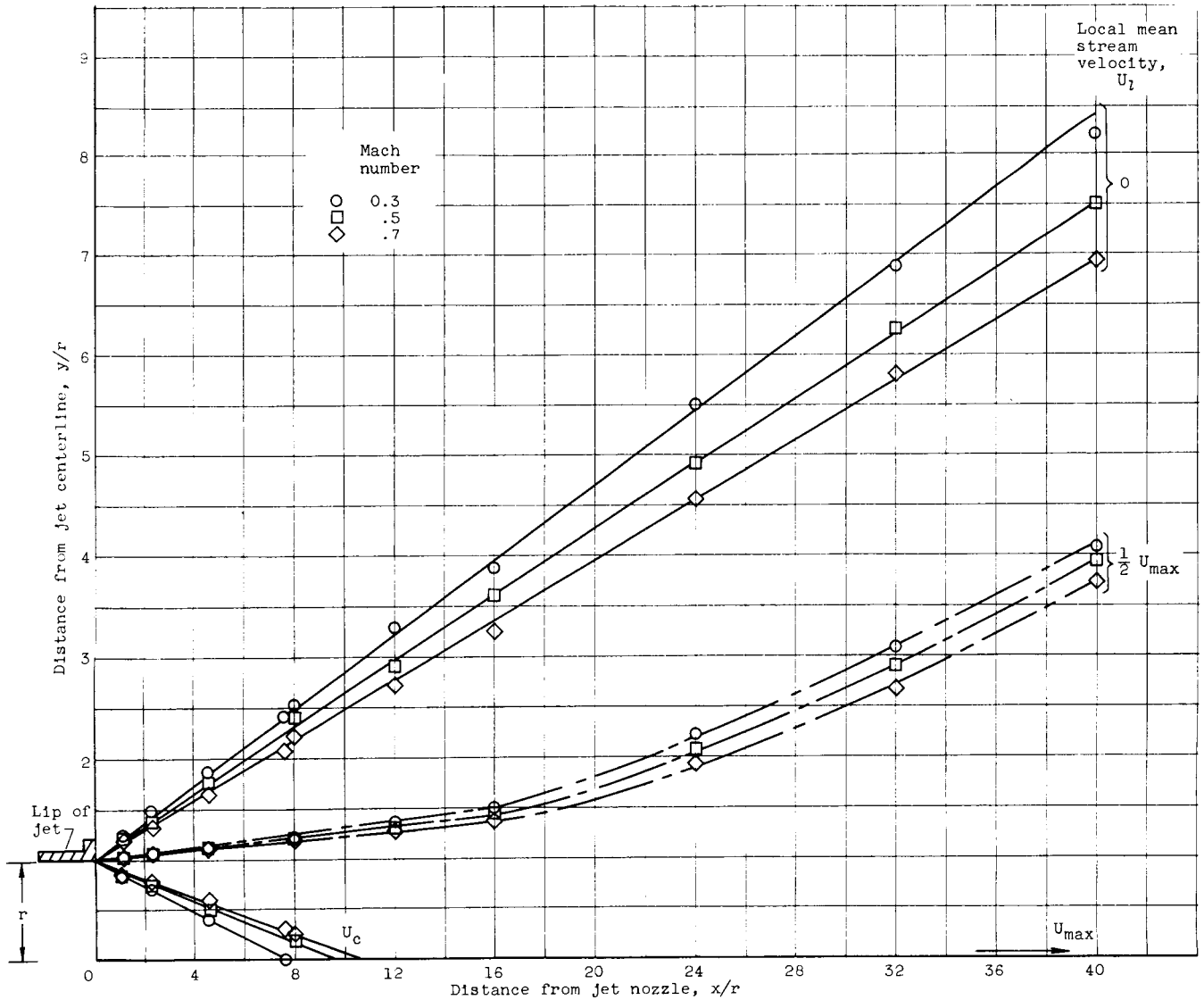

Figure 4. - Effect of potential core Mach number on boundaries of 3.5-inch-diameter jet.

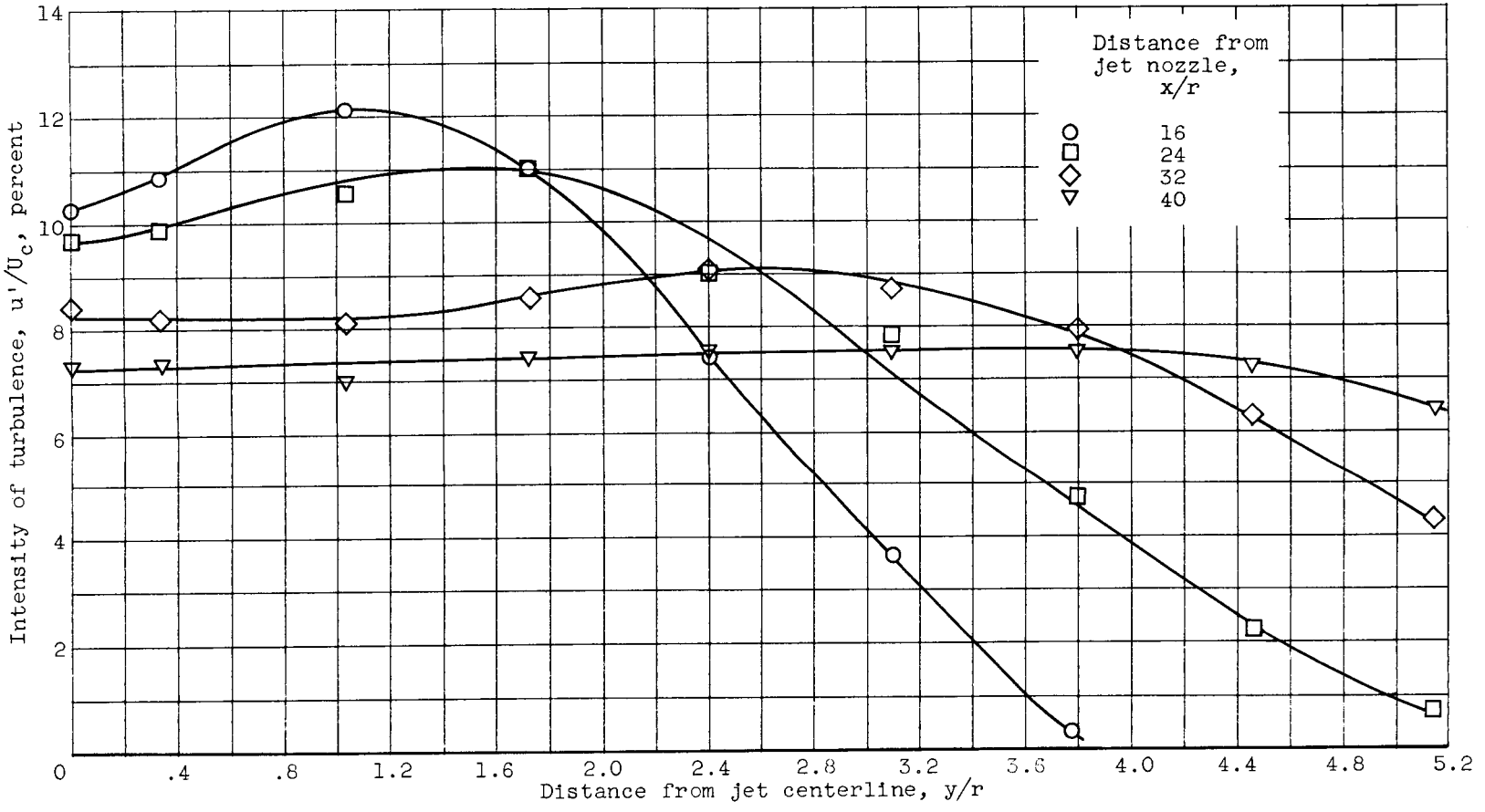

Figure 5. - Intensity of turbulence in percent of core velocity. Exit Mach number, 0.3; Reynolds number, 300,000.

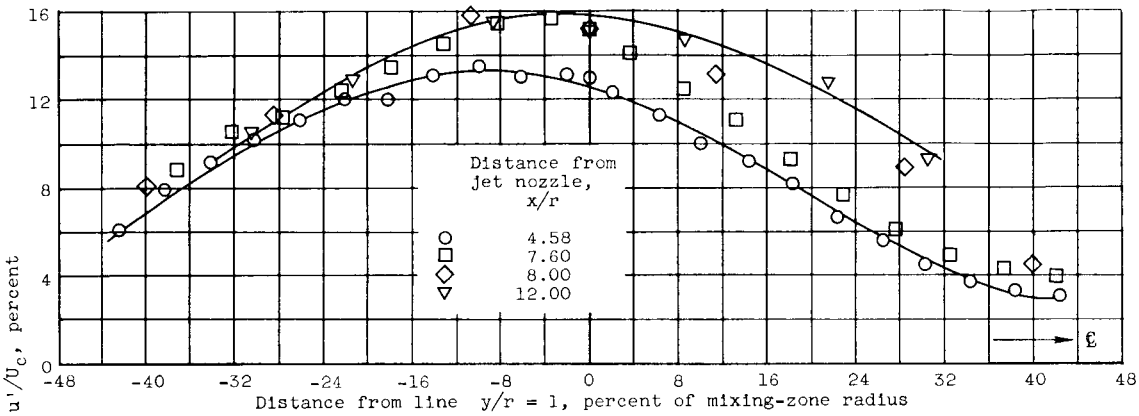

(a) Distances from jet nozzle less than 16 jet radii.

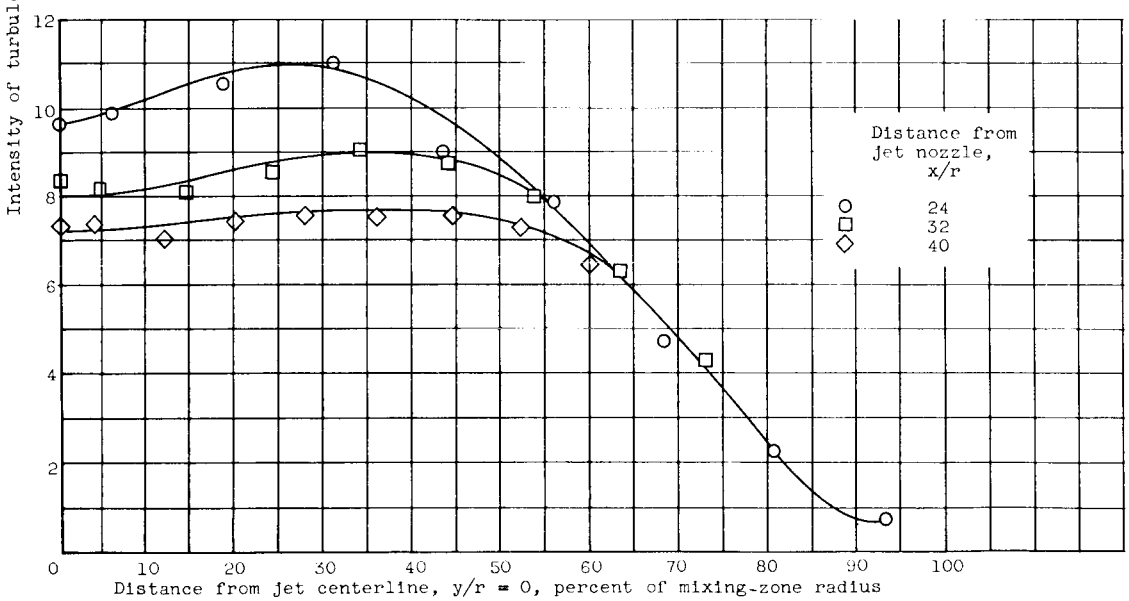

(b) Distances from jet nozzle greater than 18 jet radii.

Figure 6. - Similarity of turbulence intensity profiles. Mach number, 0.3; Reynolds number, 300,000.

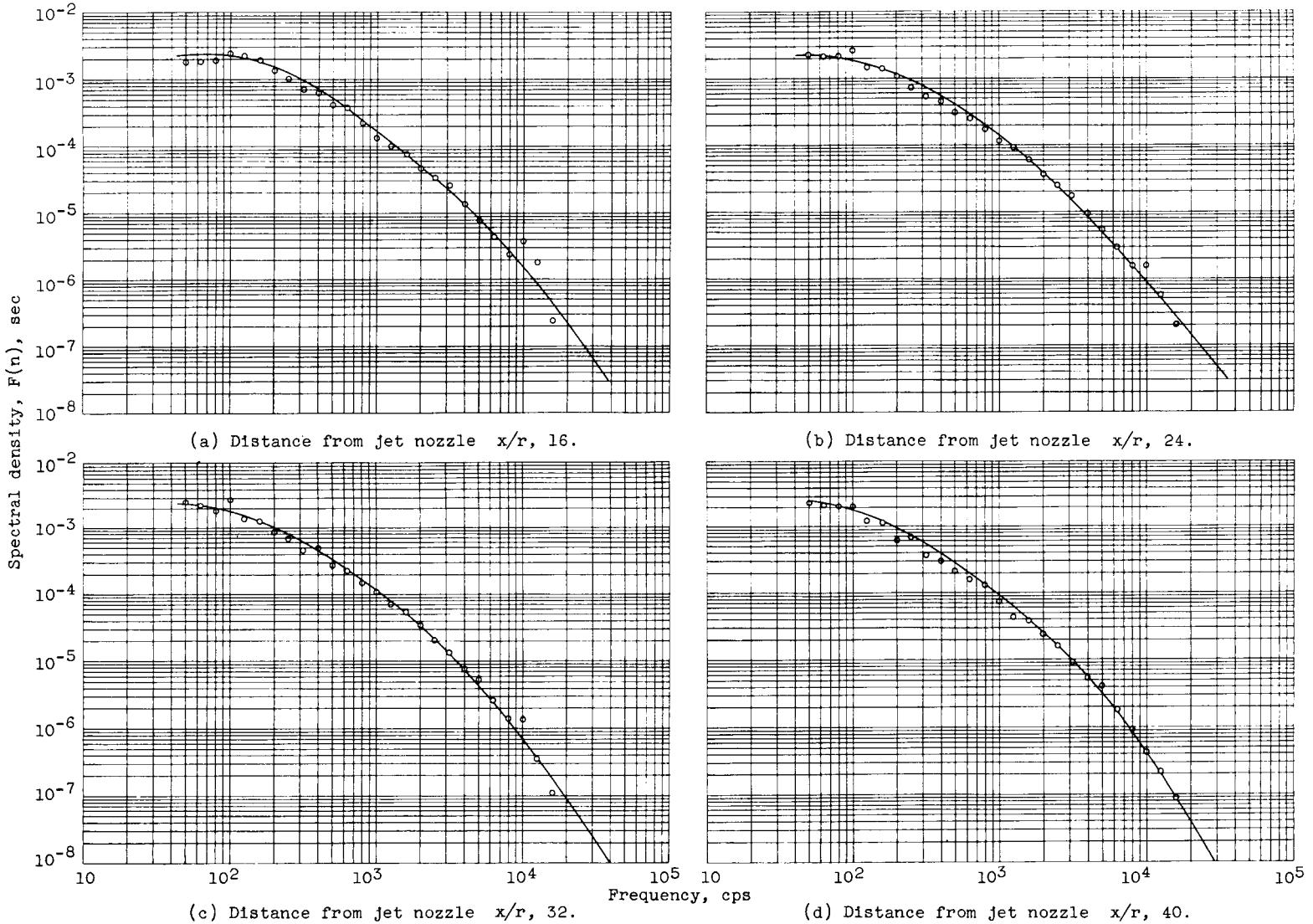

Figure 7. - Spectral density curves at various distances from jet nozzle. Distance from jet centerline y/r, 1.028; exit Mach number, 0.3; Reynolds number, 300,000.

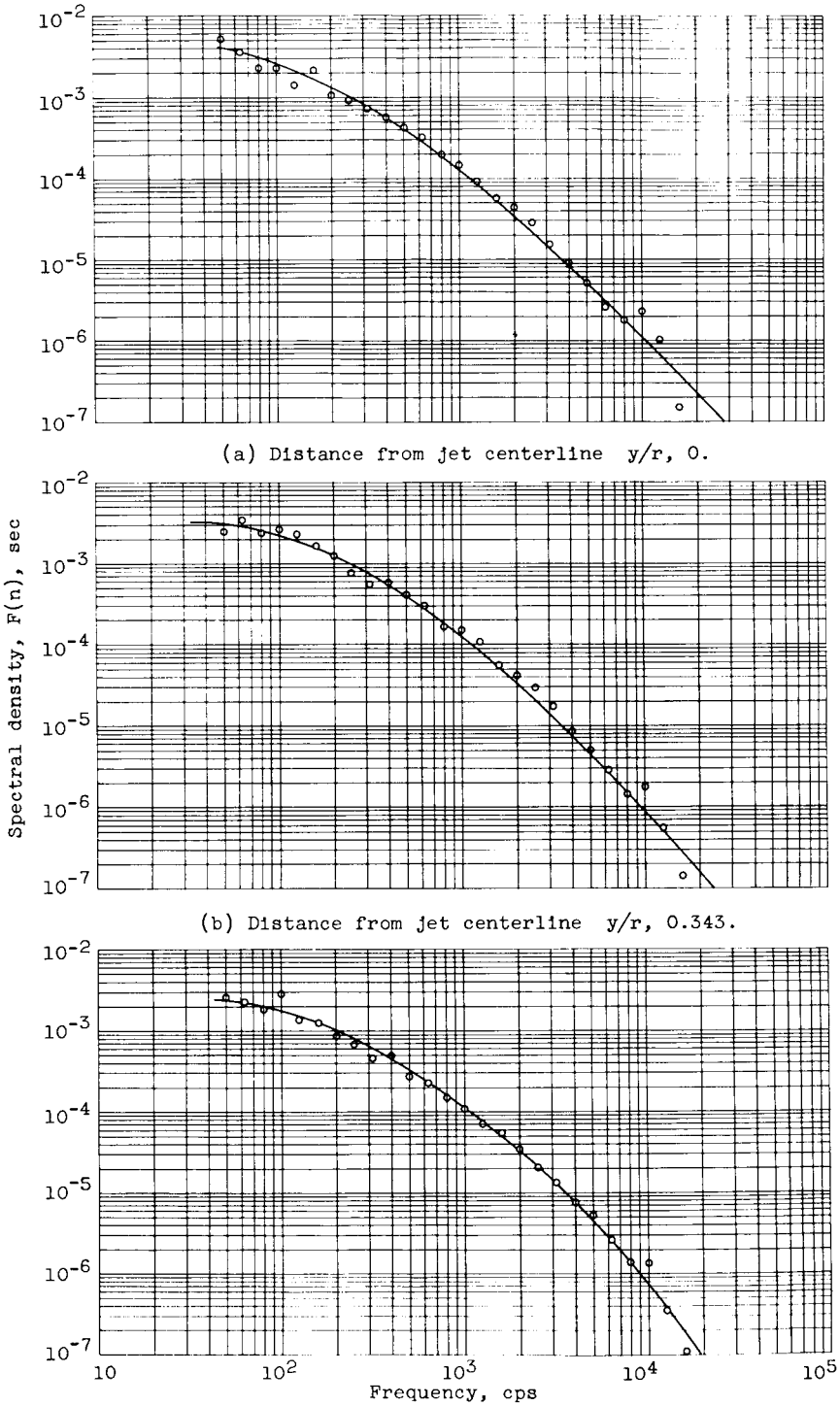

(a) Distance from jet centerline y/r, 0.

(b) Distance from jet centerline y/r, 0.343.

(c) Distance from jet centerline y/r, 1.028.

Figure 8. - Spectral density curves at various distances from jet centerline. Distance from jet nozzle x/r, 32; exit Mach number, 0.3; Reynolds number, 300,000.

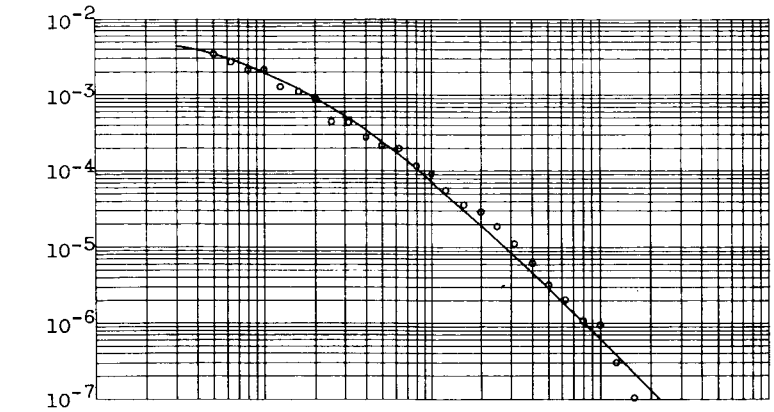

(d) Distance from jet centerline y/r, 1.715.

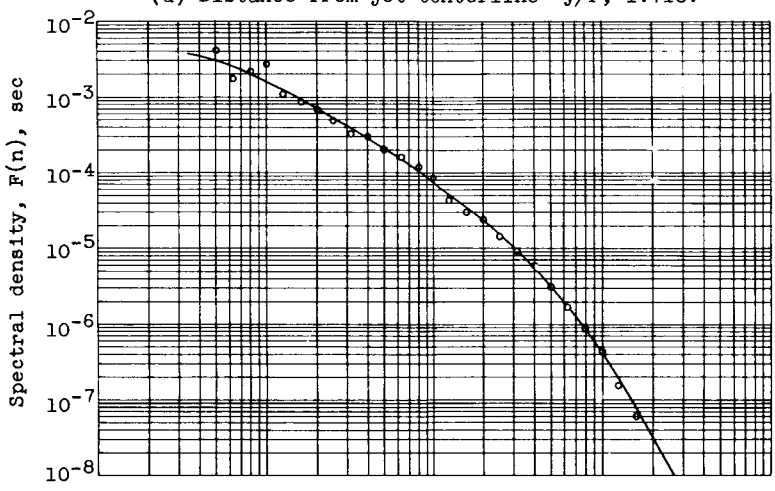

(e) Distance from jet centerline y/r, 2.400.

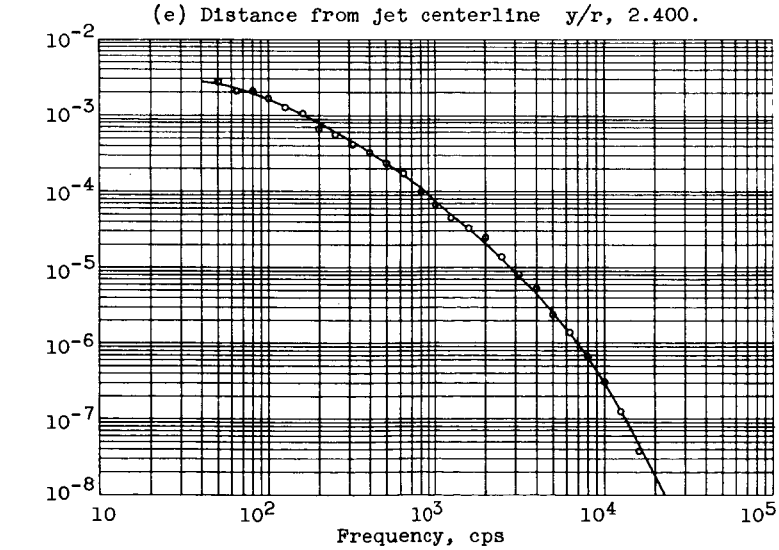

(f) Distance from jet centerline y/r, 3.088.

Figure 8. - Continued. Spectral density curves at various distances from jet centerline. Distance from jet nozzle x/r, 32; exit Mach number, 0.3; Reynolds number, 300,000.

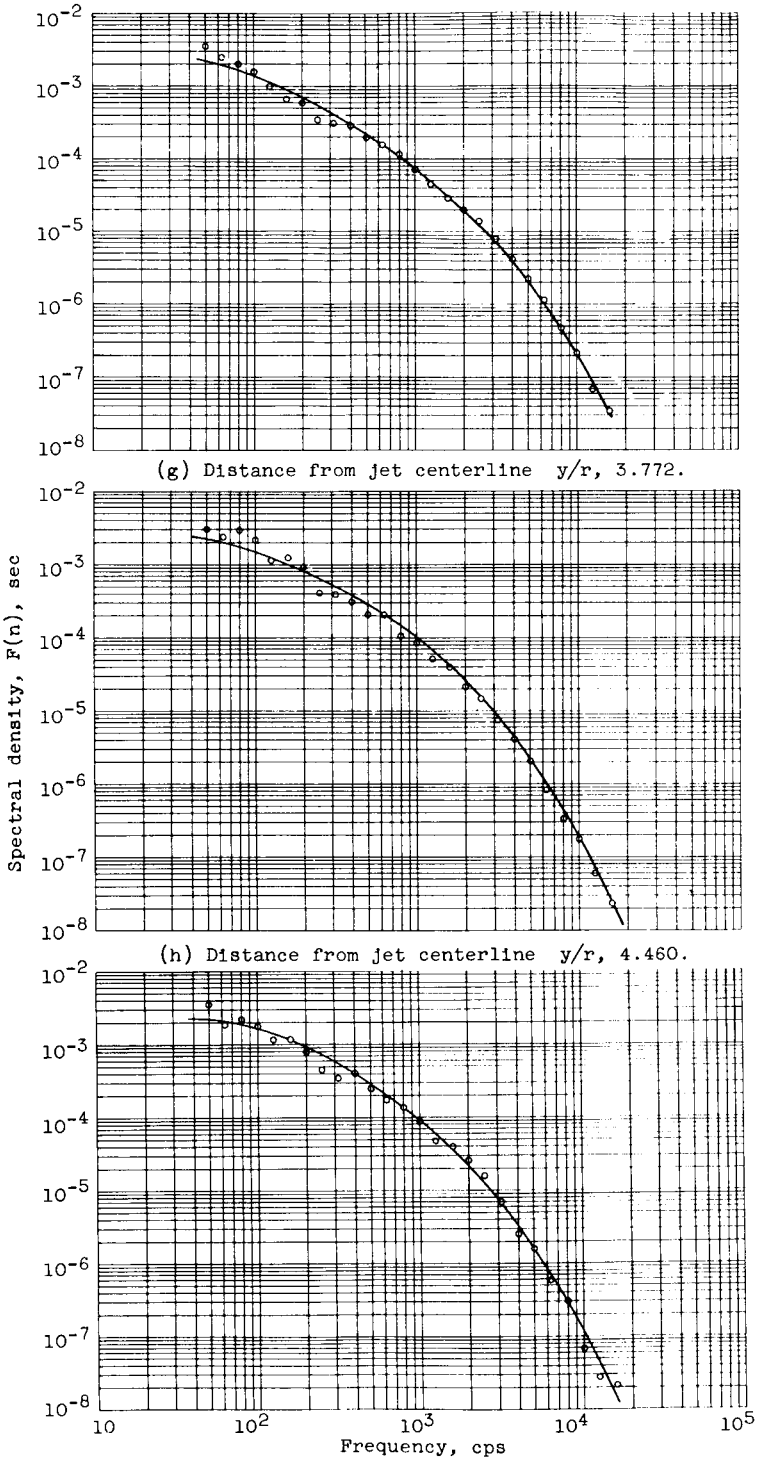

(g) Distance from jet centerline y/r, 3.772.

(h) Distance from jet centerline y/r, 4.460.

(i) Distance from jet centerline y/r, 5.143.

Figure 8. - Concluded. Spectral density curves at various distances from jet centerline. Distance from jet nozzle x/r, 32; exit Mach number, 0.3; Reynolds number, 300,000.

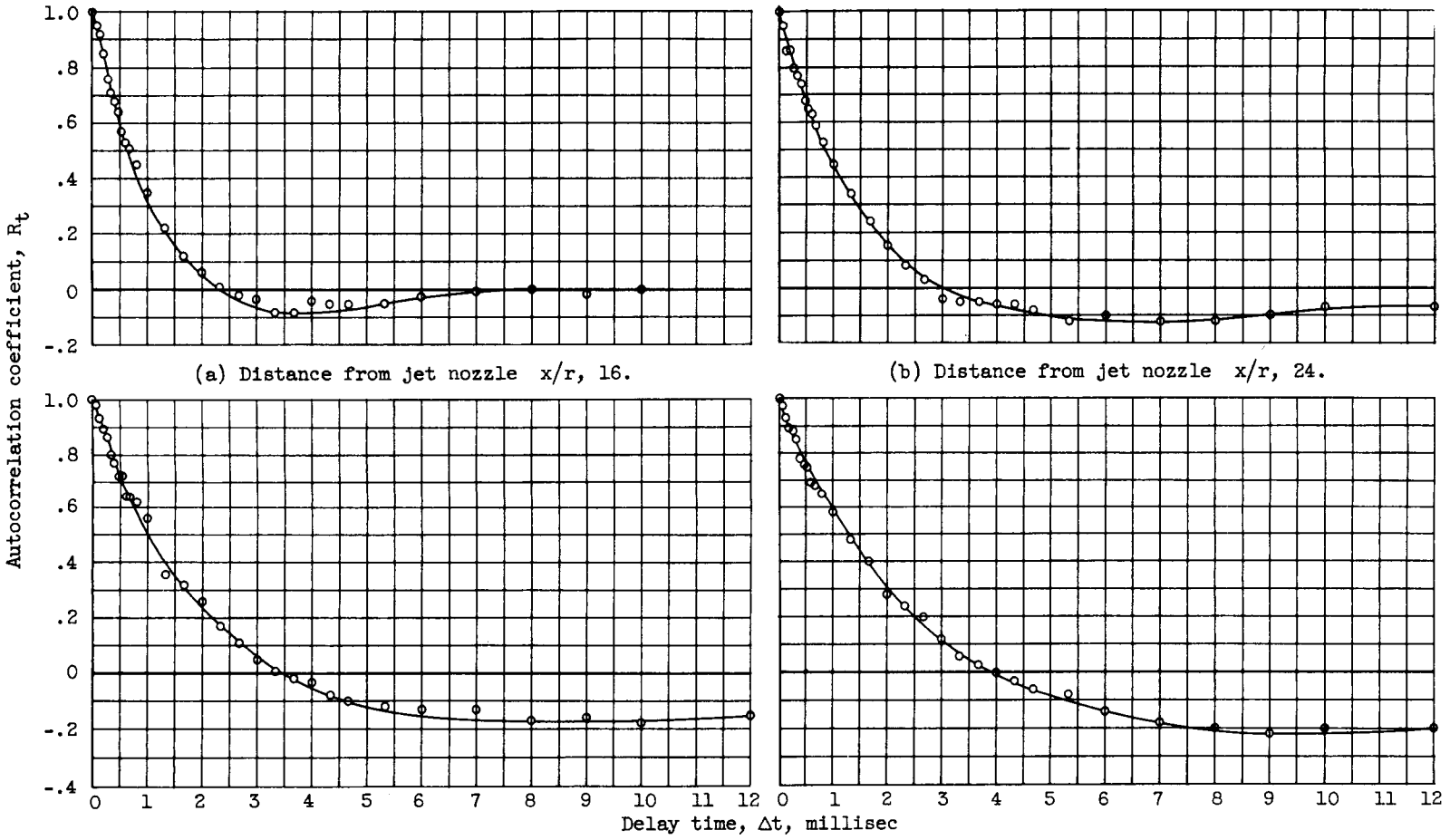

(a) Distance from jet nozzle x/r, 16.

(b) Distance from jet nozzle x/r, 24.

(c) Distance from jet nozzle x/r, 32.

(d) Distance from jet nozzle x/r, 40.

Figure 9. - Autocorrelations at various distances from jet nozzle. Distance from jet centerline y/r, 1.028; exit Mach number, 0.3; Reynolds number, 300,000.

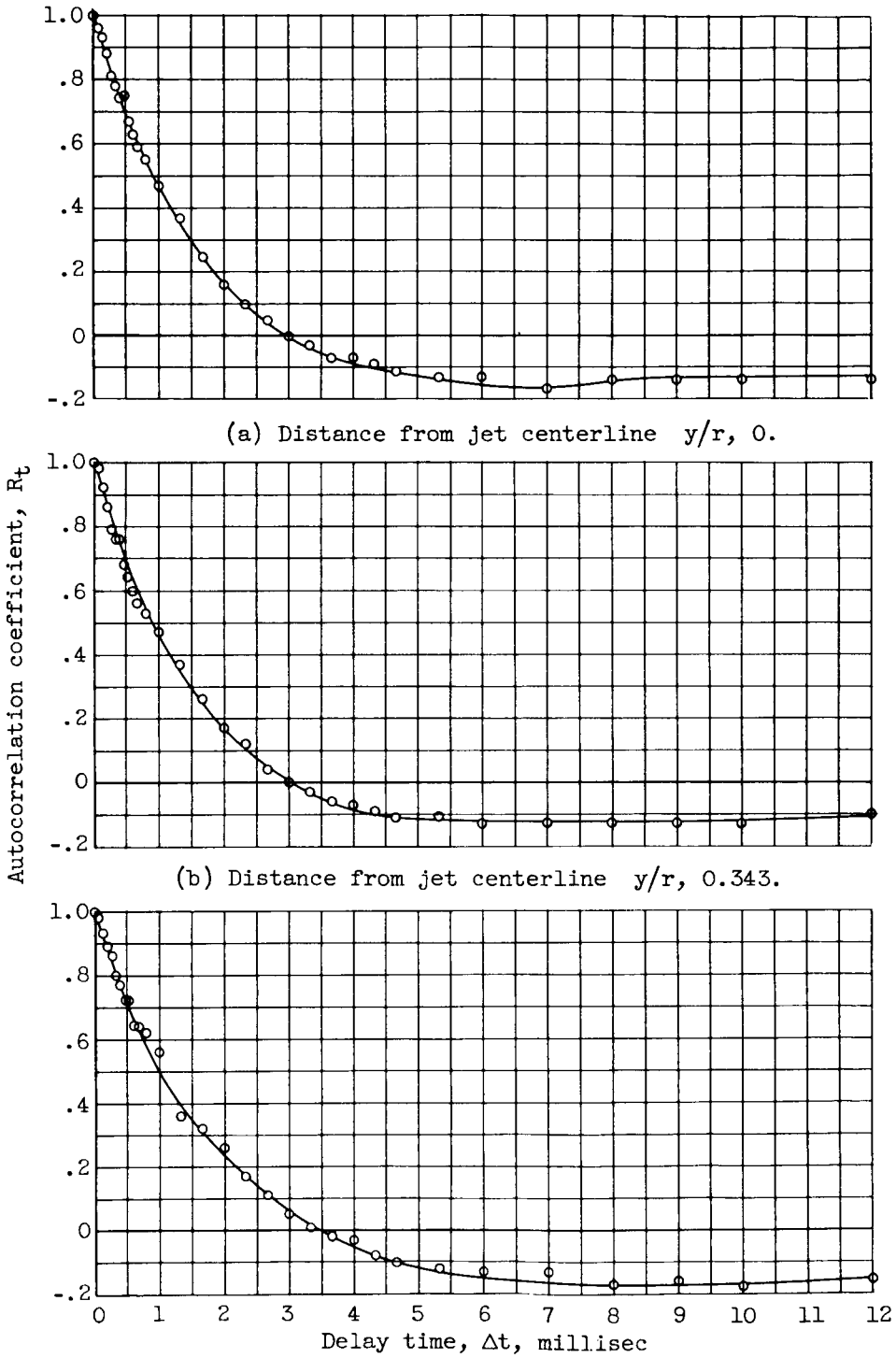

(a) Distance from jet centerline y/r, 0.

(b) Distance from jet centerline y/r, 0.343.

(c) Distance from jet centerline y/r, 1.028.

Figure 10. - Autocorrelations at various distances from jet centerline. Distance from jet nozzle x/r, 32; exit Mach number, 0.3; Reynolds number, 300,000.

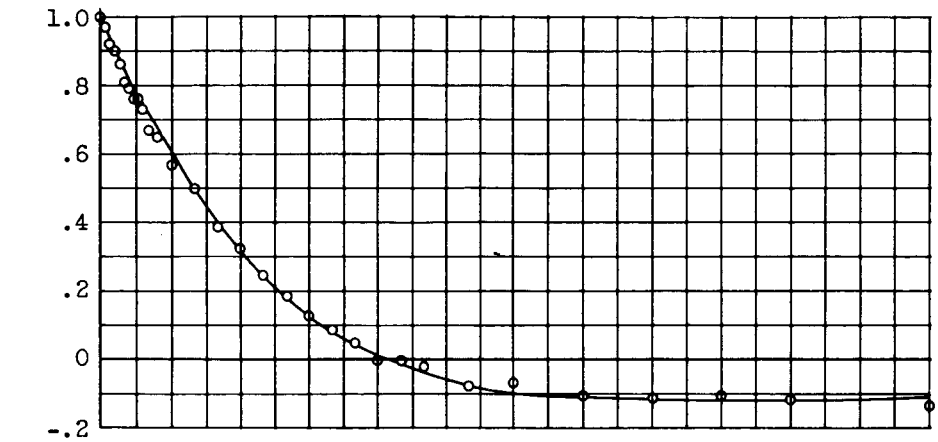

(d) Distance from jet centerline y/r, 1.715.

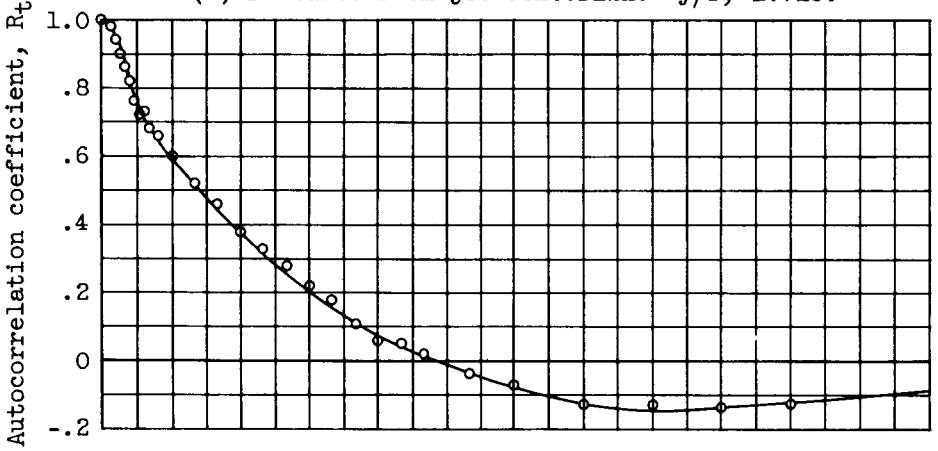

(e) Distance from jet centerline y/r, 2.400.

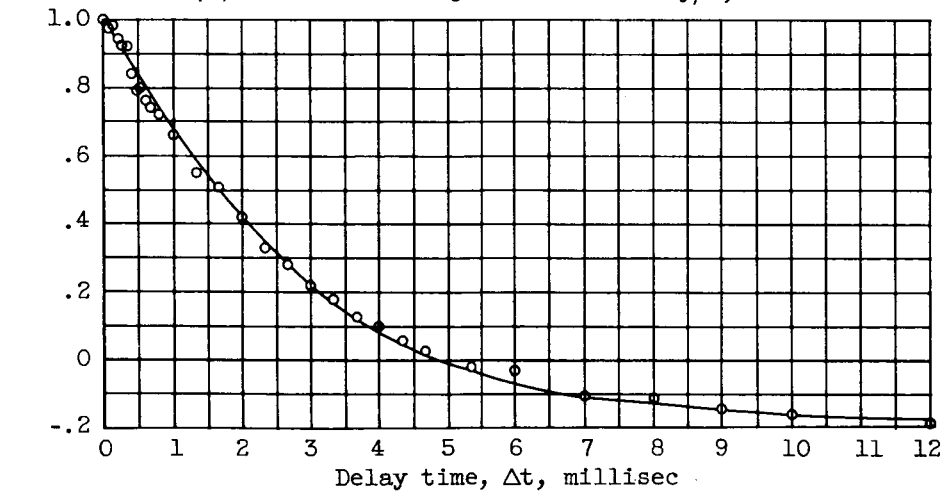

(f) Distance from jet centerline y/r, 3.088.

Figure 10. - Continued. Autocorrelations at various distances from jet centerline. Distance from jet nozzle x/r, 32; exit Mach number, 0.3; Reynolds number, 300,000.

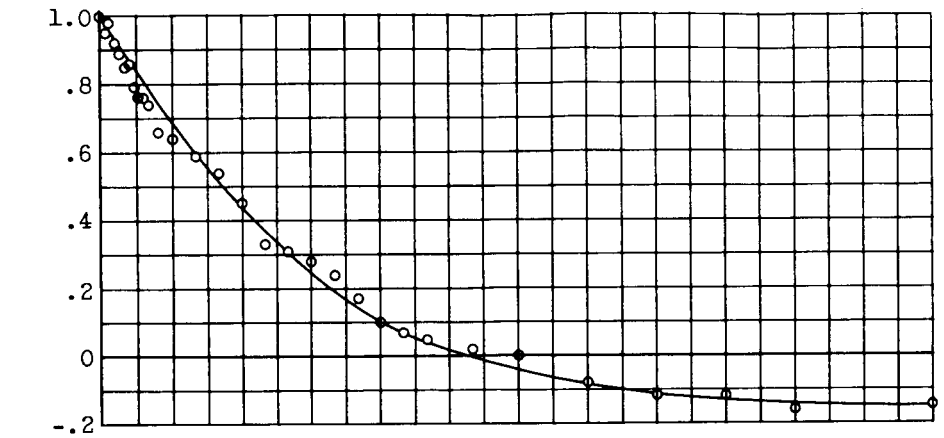

(g) Distance from jet centerline y/r, 3.772.

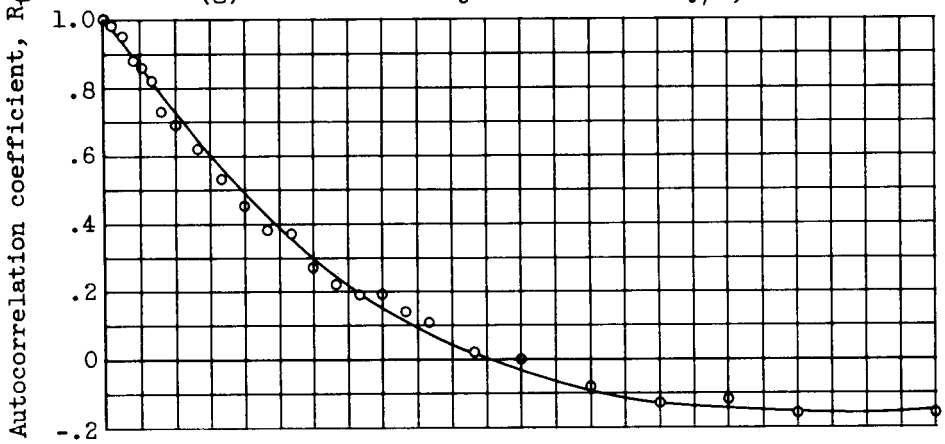

(h) Distance from jet centerline y/r, 4.460.

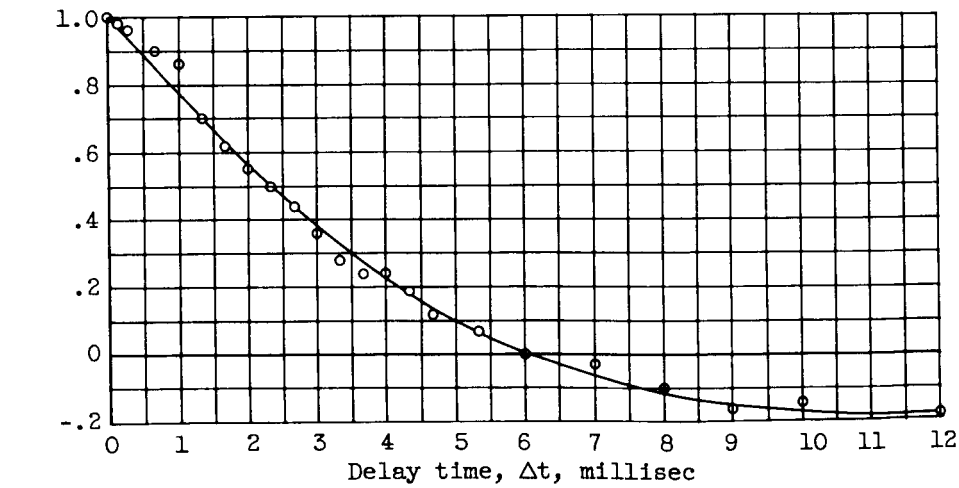

(i) Distance from jet centerline y/r, 5.143.

Figure 10. - Concluded. Autocorrelations at various distances from jet centerline. Distance from jet nozzle x/r, 32; exit Mach number, 0.3; Reynolds number, 300,000.

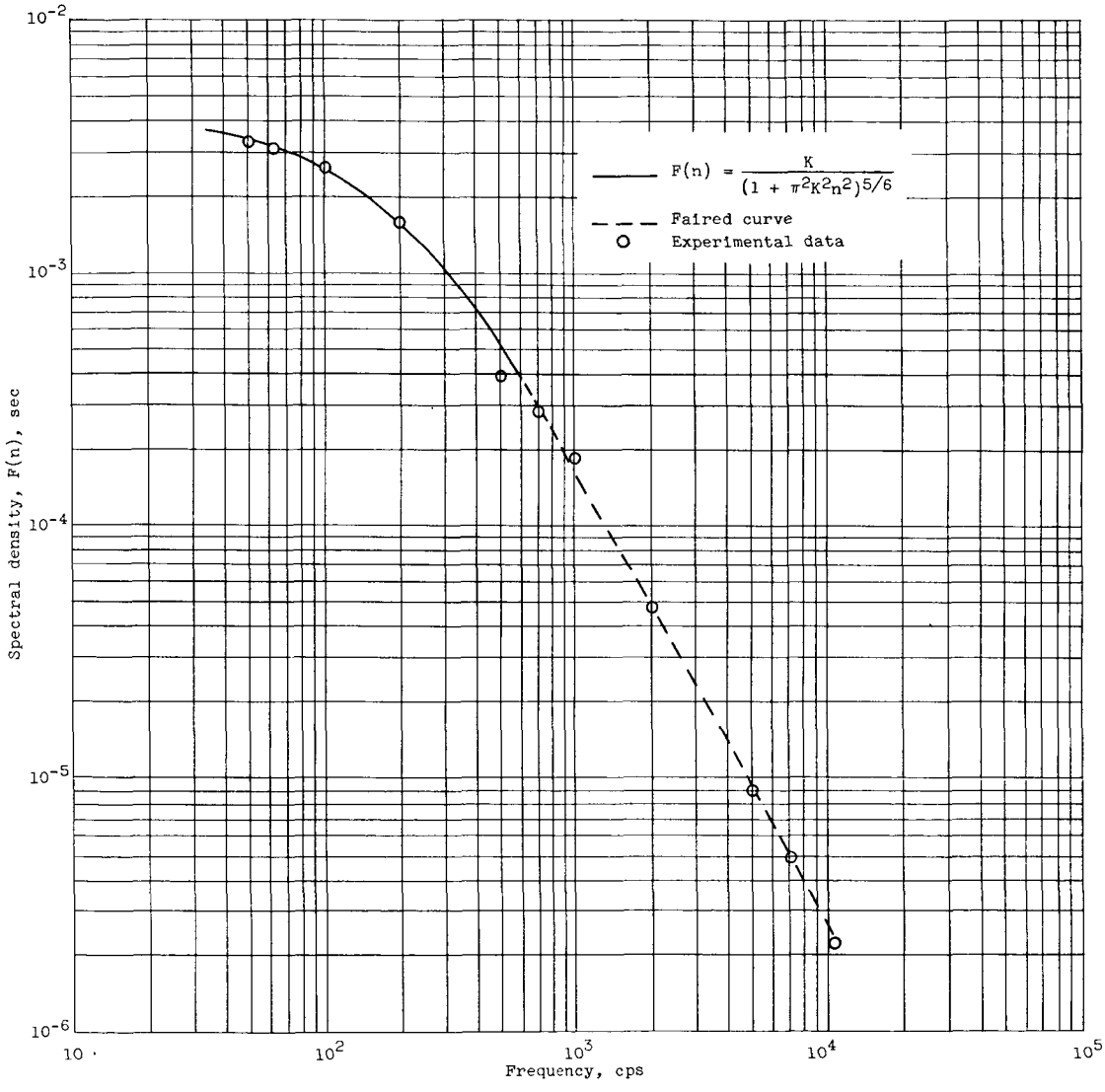

Figure 11. - Fitting spectral density data with empirical curve (ref. 9).

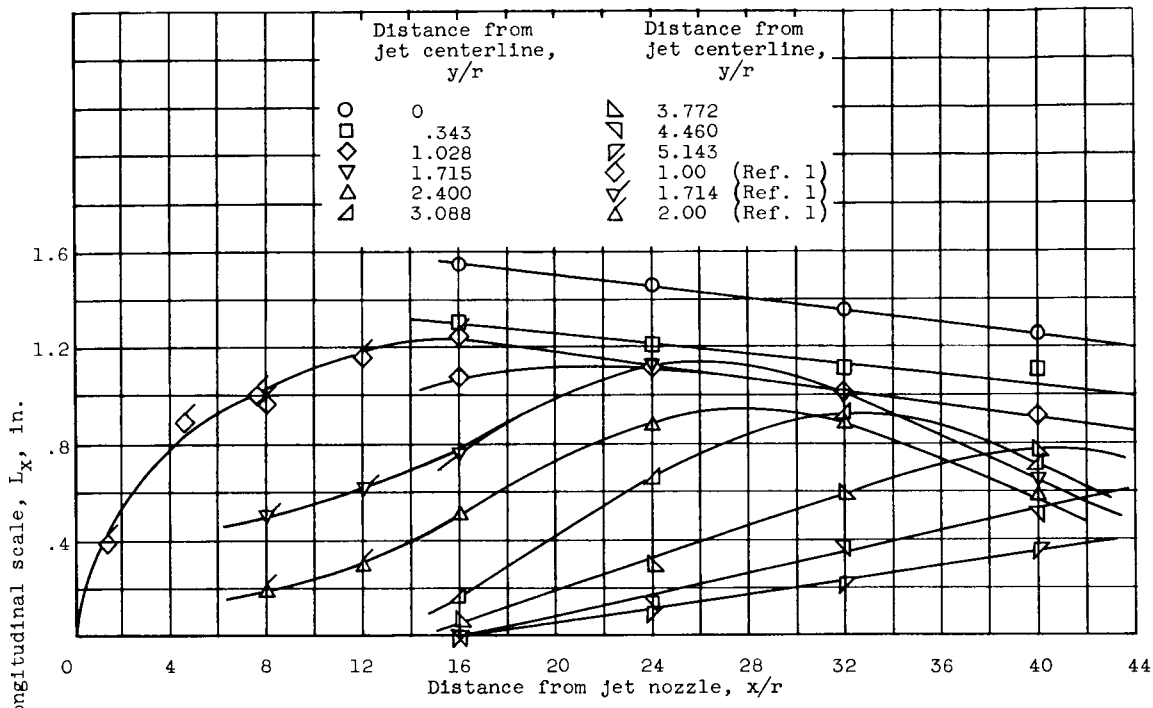

(a) Various distances from jet centerline.

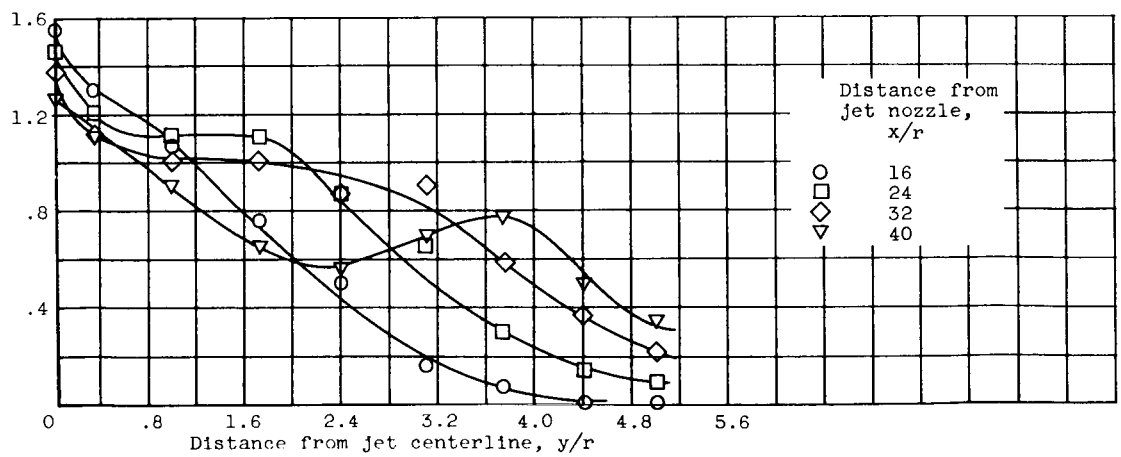

(b) Various distances from jet nozzle.

Figure 12. - Variations of longitudinal scale with location of points within jet. Exit Mach number, 0.3; Reynolds number, 300,000.